Organic Electronics 9 (2008) 775–782

Contents lists available at ScienceDirect

Organic Electronics

journal homepage: www.elsevier.com/locate/orgel

Substituting the postproduction treatment for bulk-heterojunction solar cells using chemical additives

Almantas Pivrikas *, Philipp Stadler, Helmut Neugebauer, Niyazi Serdar Sariciftci

Linz Institute for Organic Solar Cells (LIOS), Physical Chemistry, Johannes Kepler University of Linz, Altenberger Strasse 69, A-4040 Linz, Austria

ARTICLE INFO

Article history:
Received 4 April 2008
Received in revised form 13 May 2008
Accepted 15 May 2008
Available online 4 June 2008

PACS:
72.20.Jv
73.50.Gr

Keywords:
Organic solar cells
Charge transport
Recombination
Bulk-heterojunction
Postproduction treatment
Alkyl thiol

ABSTRACT

Postproduction treatment of poly (3-alkylthiophene) based bulk-heterojunction solar cells is an important and required procedure in order to fabricate organic solar cells with highest power conversion efficiencies. Postproduction treatment, by means of annealing solar cells at elevated temperatures during which an external voltage is simultaneously applied, is not very suitable for large scale production schemes due to the need for well controlled environment and involvement of flexible substrates. A faster and easier method for improving the efficiency, like a simple addition of chemicals, would be highly desirable. We have studied the effect of alkyl thiol addition into bulk-heterojunction solar cells, based on poly(3-hexylthiophene) and [6,6]-phenyl C_{61}-butyric acid methyl ester (PCBM) mixtures as reported first by Santa Barbara group [J. Peet, C. Soci, R.C. Coffin, T.Q. Nguyen, A. Mikhailovsky, D. Moses, G. C. Bazan, Appl. Phys. Lett. 89 (2006) 252105, J. Peet, J.Y. Kim, N.E. Coates, W.L. Ma, D. Moses, A.J. Heeger, G.C. Bazan, Nat. Mater. 6 (2007) 497], which gives the same final results in even higher performance of organic solar cells through increased power conversion efficiency and thus substitutes the postproduction treatment. Red-shift in optical absorption is seen in the films with alkyl thiol, resembling the absorption of thermally annealed films. Based on steady-state current–voltage characteristics and transient charge carrier extraction by linearly increasing voltage (CELIV) measurements, the conductivity of thermally annealed and films with alkyl thiol is found to be an order of magnitude higher than in films spun from pristine blends of P3HT and PCBM. Charge carrier mobility measurements indicate significant increase in carrier mobility, consistent with the improved structural order and formation of interpenetrating network between the donor and acceptor in the bulk-heterojunction solar cells.

1. Introduction

Organic photovoltaic devices offer great technological potential as a renewable source of electrical energy [3–8]. The chemical tailoring of desired physical and mechanical properties of organic materials offer advantage over the traditional inorganic semiconductor photovoltaic devices. In the best performing solid state organic solar cells reported to date [9,10], a conjugated polymer is blended with an electron accepting material, to form the bulk-heterojunction structure for efficient exciton dissociation [5]. Academic attention has focused on blends of regioregular poly(3-hexylthiophene) (P3HT) and [6,6]-phenyl C61-butyric acid methyl ester (PCBM), since these two materials show the highest power conversion efficiency in their bulk-heterojunction of around 5% [9,10]. Various studies show that the device performance is strongly related to the nanomorphology of blends, where van der Waals crystal packing of the molecules as well as the formation of nanoscale domains of the two phases is strongly dependent on the processing conditions, solvents used and finally on postproduction treatment [11–14]. A special property of P3HT is its ability to self-organize forming lamellae

* Corresponding author.
E-mail address: almantas.pivrikas@jku.at (A. Pivrikas).

1566-1199/$ - see front matter © 2008 Elsevier B.V. All rights reserved.
doi:10.1016/j.orgel.2008.05.021

structures from ordered polymer chains [10,15,16]. P3HT fibers, obtained from highly concentrated solution, are reported to increase the photovoltaic performance of polymer/fullerene solar cells [17]. In general it is possible to control the formation of a phase separated morphology with crystalline P3HT and PCBM domains inside the active layer of bulk-heterojunction solar cells can be achieved by following ways:

(1) By choosing the appropriate solvent with required boiling point for either slow or high evaporation rate [11,18,19].
(2) By reducing the drying speed of spin-coated films [20–22].
(3) By melting of bilayers [23].
(4) By thermal annealing of produced films with or without applied external voltage [12,13,24].
(5) By using chemical additives [2,25,26].

The observed correlation between domain formation and photovoltaic device performance indicates that a certain degree of phase separation of the two organic components (polymer and PCBM) is beneficial and increases the power conversion efficiency of organic solar cells. However, the alternative and simpler method of controlling the morphology of the blends is possible by adding a third material to the blend of polymer and PCBM. It has been already shown before, that the photoconductivity response is strongly increased in polymer/fullerene composites by adding a small amount of the alkyl thiol to the solution prior to the film deposition [1]. Also strongly improved photovoltaic performance and efficiency enhancement through improved morphology and interpenetrating network was observed in organic solar cells fabricated from the low band gap polymer poly[2,6-(4,4-bis-(2-ethylhexyl)-4H-cyclopenta[2,1-b;3,4-b′]-dithiophene)-alt-4,7-(2,1,3-benzothiadiazole)] (PCPDTBT) and PCBM blends [2].

In order to further to optimize the performance of organic solar cells fabricated from polymer/fullerene mixtures with alkyl thiols it is necessary to understand the influence of the additive to the molecular rearrangement as well as to the optical and electrical properties of the blends. We have chosen to use P3HT and PCBM for solar cells fabrication because these are well known and widely studied materials for efficient organic photovoltaic devices.

In this paper, we use comparative optical and electrical techniques to probe the properties of organic solar cells fabricated from regioregular P3HT and PCBM bulk-heterojunction by adding alkyl thiols. We have studied four different solar cells: (1) as produced films of P3HT and PCBM (untreated, no alkyl thiol), (2) thermally annealed films (treated, no alkyl thiol), (3) as produced films with alkyl thiol (untreated, with alkyl thiol) and (4) thermally annealed films with alkyl thiol (treated, with alkyl thiol).

Incident photon to current conversion efficiency (IPCE) is measured for all films together with the photovoltaic response. The morphology was studied using AFM, whereas current–voltage (I–V) characteristics were measured together with the charge extraction using linear increase of voltage (CELIV) and photo-CELIV technique to determine the electrical properties of these four different types of bulk-heterojunction solar cells. The results clearly show that alkyl thiol addition can substitute the post production treatment for increasing the efficiency.

2. Results and discussion

In Fig. 1 the optical absorption coefficient as a function of wavelength is shown for all four different solar cells. The increase in optical absorption upon post production treatment by annealing and simultaneous applying a constant current during treatment as has been already shown before [27–29]. The red-shift of the absorption is clearly seen for treated cells as well as for cells with alkyl thiol additive. The difference in absorption in treated and untreated solar cells, with alkyl thiol additive, is negligible indicating the final optimum structure can be achieved by the additive alone. Characteristic vibronic peaks, which are barely visible in untreated films, are clearly pronounced in treated cells and cells with alkyl thiol (at around 517 nm, 556 nm and 603 nm). The increased optical absorption allows harvesting more energy for treated cells and cells with alkyl thiol, therefore, apart from improved transport and recombination properties, these cells are expected to have better photovoltaic performance.

Current–voltage (I–V) characteristics for all cells under illumination with a solar simulator are shown in Fig. 2. To allow a comparison, the fabrication procedures were kept the same for all four types of cells. Untreated solar cells have the worst performance with the lowest short circuit current (5.2 mA/cm^2) and low fill factor. However, these cells demonstrate a relatively higher open circuit voltage (0.64 V), but, due to a low short circuit current and a low fill factor, their power conversion efficiency is only around 0.9%. Open circuit voltage has been observed to increase using the post production treatment in earlier reports [24]. This was not observed in our studies. Our as-produced untreated solar cells show slightly higher efficiency (0.9%) as compared to the earlier reported cells

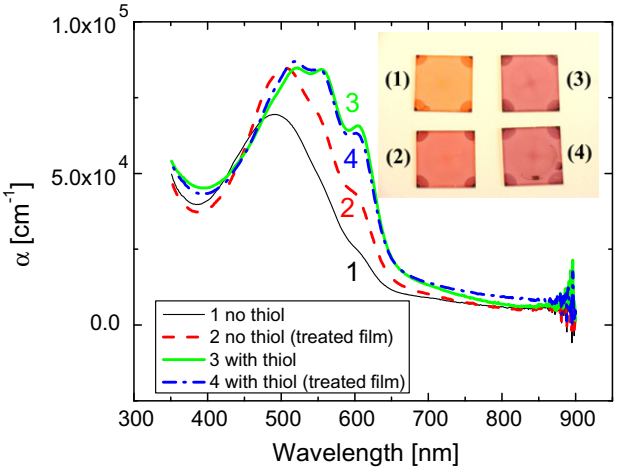

Fig. 1. Optical absorption coefficient of 4 different RR-P3HT/PCBM bulk-heterojunction solar cells: as produced (thin line), annealed (thick dashed line), thiol added (thick line), thiol added and annealed film (thick dash dot line).

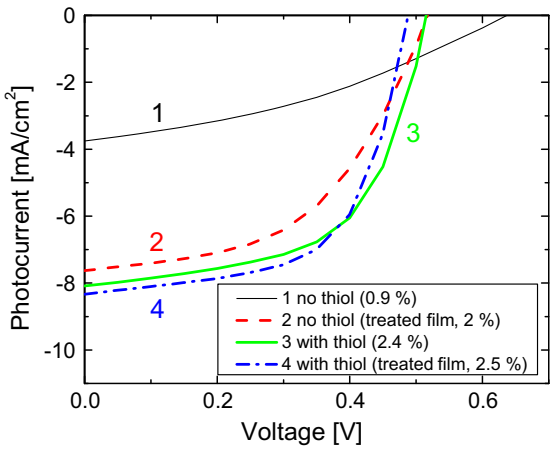

Fig. 2. Current–voltage (*I–V*) curves in the fourth quadrant of 4 different RR-P3HT/PCBM bulk-heterojunction solar cells under illumination with solar simulator (1000 W/m^2, 1.5 AM): as produced (thin line), annealed (thick dashed line), thiol added (thick line), thiol added and annealed film (thick dash dot line).

making this difference plausible. The difference in photocurrents between treated cell and cells with alkyl thiol is rather small, except that treated cells have lower fill factors and therefore slightly lower efficiency (2%) as compared to cells with alkyl thiol additive (2.4–2.5%).

Significant improvement of power conversion efficiency in treated cell and cells with alkyl thiol might arise from two effects:

(1) the increased absorption,
(2) the improved charge carrier transport and/or reduced losses, when charge carrier lifetime must be longer than the slower carrier transit time.

We have measured the incident photon to collected electron efficiency (IPCE) in all four types of cells and the results are shown in Fig. 3. Earlier studies have already shown the IPCE depends on post production treatment

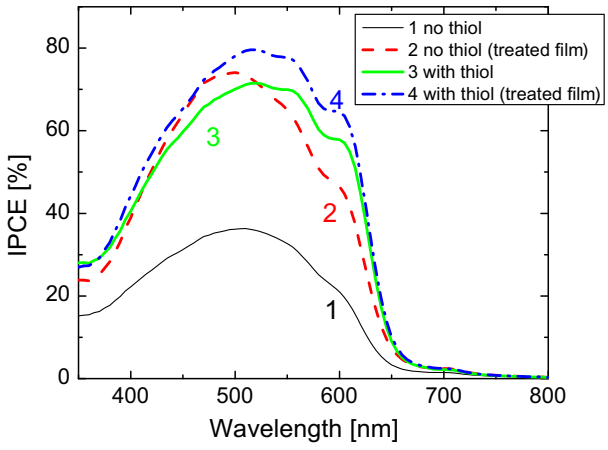

Fig. 3. Incident photon to current efficiency of 4 different RR-P3HT/PCBM bulk-heterojunction solar cells: as produced (thin line), annealed (thick dashed line), thiol added (thick line), thiol added and annealed film (thick dash dot line).

and can be up to 70–80% [24,27–30]. In all samples studied here, the IPCE is increasing at short wavelengths following the increase in optical absorption in polymer/PCBM blend, reaches a maximum and suddenly decreases following the edge of the absorption curve. The same characteristic absorption peaks seen in the optical absorption spectra (Fig. 1) are also clearly seen in the IPCE spectra. The IPCE values for the untreated cell are much smaller compared the rest of the cells, reaching a maximum of around 35%, whereas cells with treatment or alkyl thiol additives reach up to slightly below 80% IPCE. IPCE results do not allow distinguishing between improved carrier mobility and increased charge carrier lifetime, since both parameters would increase the IPCE. From the IPCE studies it can be concluded that the improvement is not only due to the increased optical absorption, but probably also due to improved transport and/or reduced recombination losses (e.g. due to longer charge carrier lifetime).

Charge transport in bulk-heterojunction solar cells usually strongly depends on the nanomorphology of the polymer/PCBM films, where the interpenetrating network formed between polymer and PCBM is created from polymer and PCBM rich phases [9,12,14,27–30]. Tapping mode AFM images (2.5 μm × 2.5 μm) of all studied cells are shown in Fig. 4. In cells without alkyl thiol the coarse morphology is stronger in treated films, with the surface roughness staying similar (on the same 5 nm scale). Both treated and untreated cells with alkyl thiol show much coarser surface as compared to the cells without alkyl thiol. Apparently, as it has already been shown before [2], polymer and PCBM rich phases is advantageous for charge transport and photovoltaic performance for films with alkyl thiol additive. As has been already shown before, the fact that addition of alkyl thiols strongly influences the structure of the interpenetrating network most likely is the reason for the improved IPCE and power conversion efficiency. The electron and hole transport to the electrodes might be improved, since pronounced polymer and PCBM phases will create well defined pathways for the transport of the respective charges.

Dark current–voltage (*I–V*) curves recorded for all 4 different solar cells are shown in Fig. 5a. The dark current, shown in the region of negative applied voltage, representing the reverse bias (positive voltage on Al, negative on ITO), is similar for all cells. The current in forward bias is much larger compared to the reverse bias current. The rectification ratio for the treated cells and for cells with alkyl thiol is more than two orders of magnitude, whereas for untreated cells the rectification ratio is one order of magnitude less compared to other cells.

Due to the different nanomorphology of the interpenetrating network, the dark conductivity is expected to increase in the cells with higher conversion efficiency, because of improved conductivity of the films (assuming the injection is not limited by the contact). This effect has been already observed in the case of postproduction treatment [24,30]. The dark injection current (at large forward bias) is much lower in untreated cells without alkyl thiol, suggesting that either the carrier mobility or equilibrium carrier concentration is smaller compared to treated cells and cells with alkyl thiol:

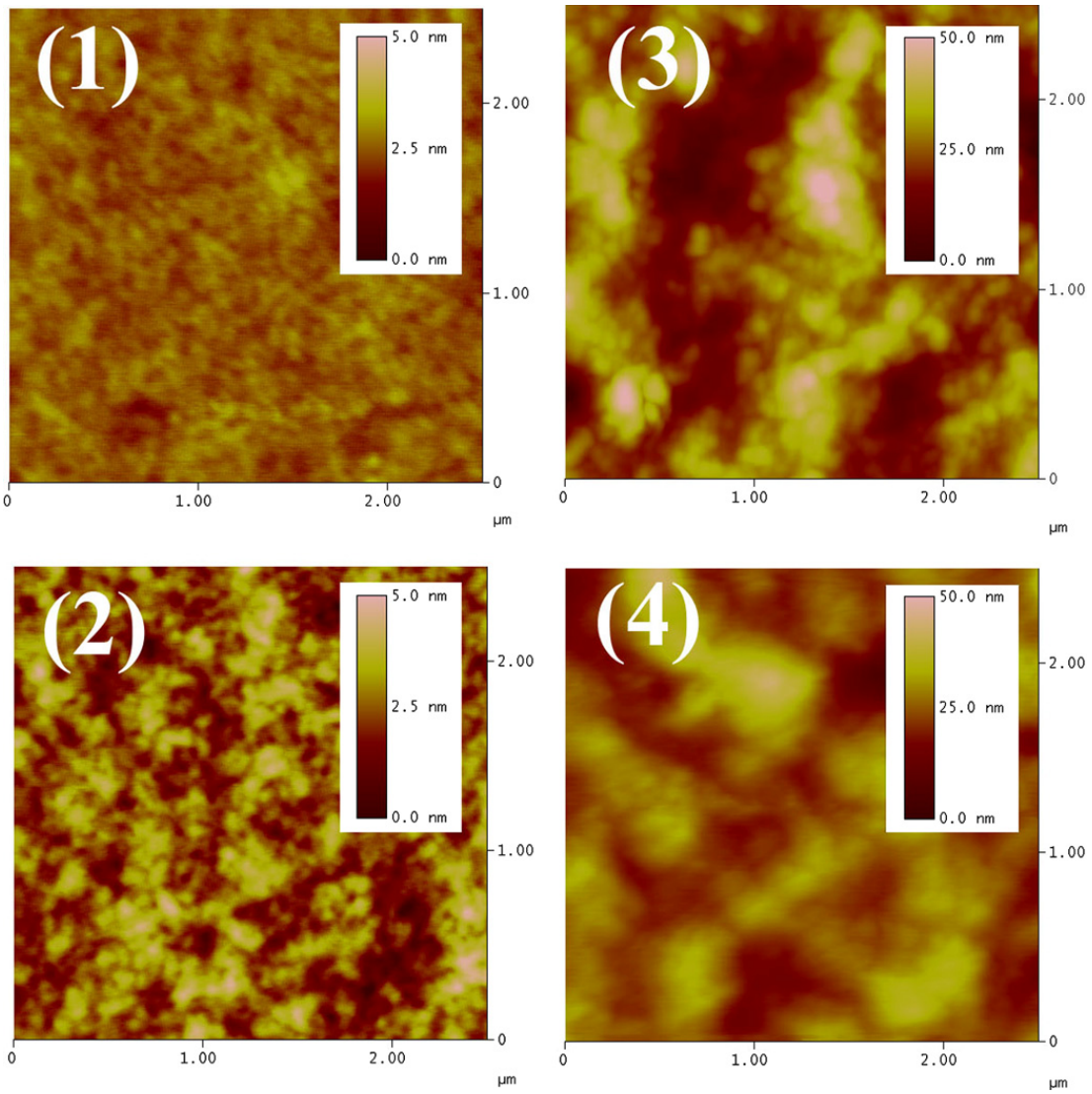

Fig. 4. Tapping mode AFM images of 4 different RR-P3HT/PCBM bulk-heterojunction solar cells: as produced (1), annealed (2), thiol added (3), thiol added and annealed film (4). The RMS surface roughness for all solar cells is 0.2 nm (cell 1), 0.6 nm (cell 2), 7.1 nm (cell 3), and 4.3 nm (cell 4).

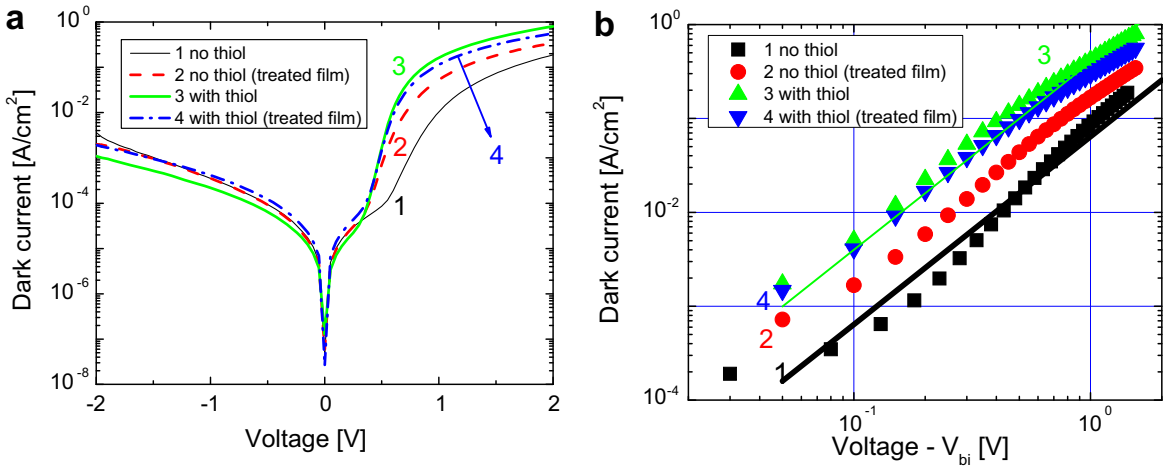

Fig. 5. Dark current–voltage (*I*–*V*) curves (a) and same dependencies plotted in log–log scale with built-in voltage subtracted (b) of 4 different RR-P3HT/PCBM bulk-heterojunction solar cells: as produced (thin line), annealed (thick dashed line), thiol added (thick line), thiol added and annealed film (thick dash dot line). Straight lines (thick for sample 1 and thin for sample 3) are calculated ideal Mott's space charge limited currents using carrier mobility at long time obtained from photo-CELIV (Fig. 7).

$$(j = en\mu_n E + ep\mu_p E), \quad (1)$$

where j is the current density, e is electron charge, n and p are the electron and hole concentration, respectively, μ_n and μ_p are the electron and hole mobilities, respectively, and E is the electric field). In principle, another possibility for a smaller dark current in forward bias in untreated cells without alkyl thiol could be due to a contact limited injection. The post production thermal treatment and/or the alkyl thiol addition could have altered the contact properties between the interpenetrating network and the electrode. However, treated cells without alkyl thiol (which also have high dark injection current) were annealed without the aluminum electrode, which was thermally evaporated afterwards. Therefore, at least Aluminum electrode interface cannot be responsible for the lower dark current in forward bias in the untreated cells.

In Fig. 5b the same dark current–voltage curves with subtracted built-in voltage (taken from the open circuit voltage of the I–V curves under illumination) are plotted in log–log scale in order to characterize the current–voltage dependence. For voltages above 1 V the current seems to approach a square dependence but deviates at larger voltages in treated cell and cells with alkyl thiol. As it will be shown later from Fig. 6a, at given geometry and intrinsic conductivity, a space charge limited current already dominates at 1 V in all our cells, due to low intrinsic carrier concentration (SCLC condition is reached when the charge on the electrodes (CU) is larger than the charge present inside the film, $Q > CU$).

The straight line in Fig. 5 shows the calculated SCLC current for sample 1 and sample 3, where the carrier mobility is taken at longest delay times from the photo-CELIV technique (shown below in Fig. 7) because of the dispersive nature of charge transport in organic materials. The following equation was used to calculate SCLC [31]:

$$j = \frac{9}{8}\varepsilon\varepsilon_0\mu\frac{U^2}{d^3}, \quad (2)$$

where ε and ε_0 are the relative and vacuum's dielectric permittivity respectively, U is applied external voltage and d is the film thickness. The dark current measured in untreated solar cells (Fig. 5b) is lower as compared to treated cell and cells with alkyl thiol, so is the carrier mobility (at longer times) as shown in Fig. 7. The calculated SCLC values and current measured from I–V curves are in rather good agreement within the experimental error, showing that the photo-CELIV experiment rather well estimates the steady-state carrier mobility. It is important to note that usually in steady-state space-charge-limited conduction models [31] a carrier transport with carrier mobility independent on the electric field is assumed, which is rarely the case in disordered materials like in solution processed films.

In order to find out whether the increased dark current in treated cell and in cells with alkyl thiol is due to higher carrier intrinsic concentration (due to doping, impurities or similar effects) or due to improved charge carrier mobility, we have studied the cells using dark charge carrier extrac-

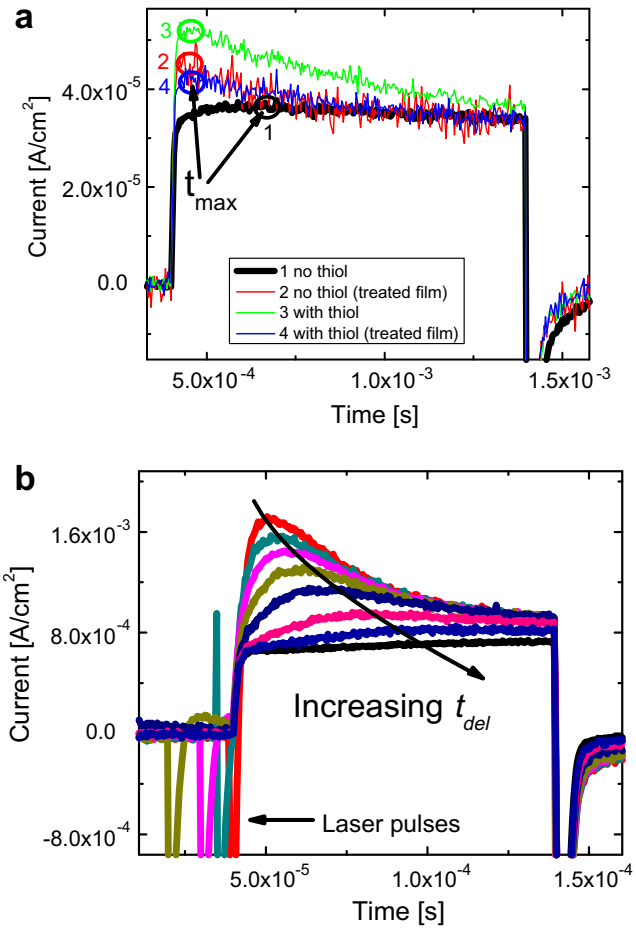

Fig. 6. (a) CELIV dark current transient response to an applied triangle-shaped voltage pulse in reverse bias of 4 different RR-P3HT/PCBM bulk-heterojunction solar cells: as produced (thin line), annealed (thick dashed line), thiol added (thick line), thiol added and annealed film (thick dash dot line). Circles mark the position of current extraction maximum (t_{max}) for all four different type of films. (b) Photo-CELIV current transients recorded for various delay times t_{del} between the laser and triangle-shaped voltage pulses. The extraction maximum time shift is guided with an arrow.

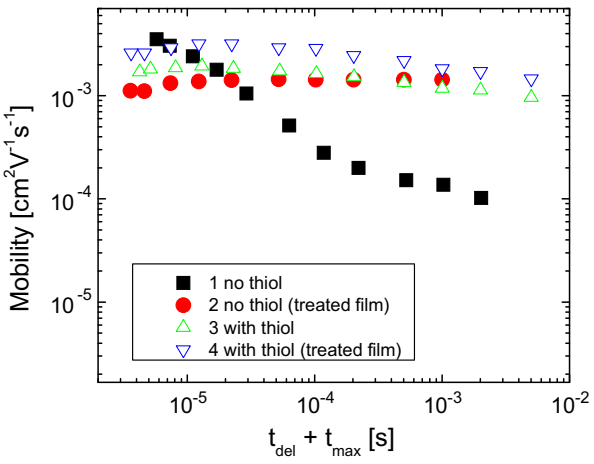

Fig. 7. Charge carrier mobility of 4 different RR-P3HT/PCBM bulk-heterojunction solar cells: as produced (filled squares), annealed (filled circles), thiol added (open up-pointing triangles), annealed film with thiol (open down-pointing triangles).

tion by linearly increasing voltage (dark CELIV) technique [32]. This technique allows to measure the charge carrier concentration and the mobility simultaneously [33]. The dark CELIV current transients are shown in Fig. 6a. In CELIV experiments a triangle-shaped voltage pulse is applied in reverse bias. The film acts as a capacitor, and the current is measured with an Oscilloscope's load resistance forming all together a differentiating RC circuit. The current response would show a constant current pulse if the capacitor would be ideal without mobile charges between the capacitor plates. However, if there is an intrinsic carrier concentration inside the film, the dark current response would be seen as a conductivity current on top of the constant capacitive displacement current step. The charge mobility can then be estimated from the current extraction maximum and charge concentration is estimated and by integrating the current over time [32,33]. The current transient response shown in Fig. 6a is different for the untreated cells without alkyl thiol and the other cells. At the initial time the current is rapidly increasing in the treated cell and cells with alkyl thiol, whereas later the current decreases forming an extraction maximum (t_{max}). The extraction current in the untreated cell is much smaller and the extraction maximum is at longer times showing less equilibrium charge with slower mobility in the untreated solar cells.

From Fig. 6a the equilibrium (intrinsic) charge concentration is estimated $5.6 \times 10^{14}\,cm^{-3}$ in the untreated sample (1), $1.3 \times 10^{15}\,cm^{-3}$ in the treated sample (2), $3.8 \times 10^{15}\,cm^{-3}$ in the untreated sample with thiol (3), and $1.7 \times 10^{15}\,cm^{-3}$ in the treated sample with thiol (4). The charge present in the film are calculated to be below 4×10^{-10} C, whereas the charge due to the geometrical capacitance at 1 V is around 3×10^{-9} C (for contact area around 5 mm^2). Therefore, the charge on the electrodes for all samples (samples were made with similar geometries) at 1 V is much larger than the equilibrium intrinsic charge stored in the film, which justifies using the model of a space charge limited current (as discussed above). This observation is in agreement with high purity organic semiconductors where the steady state SCLC is easily reached at rather low applied external electric field [34,35].

For measuring the mobilities of photogenerated charge carriers, we have used the photo-CELIV technique [36]. This technique is able to probe dispersive transport which is typical in all disordered materials. As an additional advantage, the charge carrier mobility can be measured in <100 nm thin films, where typical time-of-flight (TOF) technique is not applicable [37]. The main advantage of this method is that it allows measuring the carrier mobility and density simultaneously. The charge carriers are photogenerated with a short laser light pulse prior to their extraction with a triangle-shaped voltage pulse. The delay between the laser and triangle voltage pulses (t_{del}) is changed and the current transients are recorded in the oscilloscope for different delay times. Experimentally measured photo-CELIV transients were recorded for all four types of solar cells and where the transients for untreated solar cells without thiol are shown in Fig. 6b. The charge carrier mobility is then estimated using the following equation:

$$\mu = \frac{2d^2}{3At_{max}^2}, \tag{3}$$

where A is the slope of triangle-shaped voltage pulse.

Fig. 7 shows the charge carrier mobilities for all four types of films experimentally measured from the photo-CELIV current transients. Mobility is plotted as a function of time, which is the sum of both the delay time between the laser pulse and triangle voltage pulse and the extraction maximum. The carrier mobility in the untreated film without alkyl thiol has a very strong time-dependence, whereas the carrier mobilities in the other films show a rather time-independent behavior. Interestingly, the carrier mobility at very short time is very similar in all films. In untreated films, this similar value might arise from the unfinished carrier relaxation in the broad density of states (DOS). The relaxation of the photogenerated charge carriers and the carrier mobility saturates when DOS has a Gaussian distribution, as described by Bässler's theory of charge transport in disordered organic materials [38,39]. At longer times, when the carrier mobility approaches the dynamic equilibrium, the difference between the untreated film and the rest of the films becomes larger.

In CELIV experiments the measured current is determined as a sum of both faster and slower carrier mobilities as shown in Eq. (1), therefore, the plotted mobility in Fig. 7 is presumably from the faster carriers [40]. The dark injection current will be mostly dominated by carriers with faster mobility, so we can use the photo-CELIV mobility to calculate the SCLC current which is shown as a line in Fig. 5b).

3. Conclusions

Addition of alkyl thiols to P3HT/PCBM solar cells results in improved photovoltaic performance and efficiency compared to pristine untreated and even to thermally annealed cells. Therefore, substitution of postproduction treatment of bulk-heterojunction solar cells can simplify the solar cell fabrication process. Solar cells fabricated with alkyl thiol show red-shifted absorption compared to untreated and even to thermally annealed cells. In addition, the optical absorption coefficient increases in the cells with alkyl thiol. Both effects allow for a better overlap with the solar spectrum and for a larger portion of energy absorbed. IPCE spectra and current–voltage characteristics show a large difference between untreated solar cells without alkyl thiol and the cells with the additive. In this study the power conversion efficiency in unoptimized solar cells with alkyl thiol was found to be 2.5% whereas for the untreated P3HT/PCBM cells around 0.9% (under AM1.5 standard illumination conditions) were obtained. We found that thermal treatment and alkyl thiol addition strongly increases dark current, which is mainly due to improved charge carrier mobility, as seen from time resolved carrier mobility measurements with photo-CELIV. Untreated solar cells show much a strong decay of carrier mobility with time. Treated cells and cells with alkyl thiol mobility is nearly time-independent suggesting reduced losses. The relaxed carrier equilibrium mobility is in rather good agreement with

the steady state space charge limited current in the current–voltage characteristics. The improved carrier equilibrium mobility is explained by the differences in the morphology of the cells. Treated cells and cells with alkyl thiol, show improved interpenetrating network and well defined pathways for the electron and hole conduction to the electrodes.

4. Experimental

Bulk-heterojunction solar cells were prepared according to the following procedure: indium tin oxide (ITO) coated glass substrates with surface resistance of $\sim$15 square^{-1} (purchased from Merck) were cut to square pieces 1.5 cm $\times$ 1.5 cm and approximately half of ITO was chemically etched away. Substrates were then first mechanically cleaned using Kodak lens cleaning tissue and afterwards washed in the ultrasonic bath using organic solvents and dried in a nitrogen flow. A thin layer of high quality poly(3,4-ethylenedioxythiophene)-poly(styrenesulfonate) (PEDOT:PSS) in aqueous solution (purchased from Bayer AG) was spin-coated on the substrates using 2000 RPM spin-coater speed. The thickness of PEDOT is below 50 nm. Substrates with PEDOT were annealed on the hotplate for several minutes at 120 °C. The photoactive layer of polymer and PCBM was spin-coated on top with typical thicknesses of 100–200 nm. Four different photoactive layers were used in the experiment: first 10:8 mg/ml ratio of P3HT and PCBM in toluene was prepared, well dissolved in the ultrasonic bath. The solution was separated into two glass bottles and 5% by volume of *n*-octylthiol was added to one of the solutions. Both solutions were filtered through 0.45 μm filter and deposited on to the prepared substrates: 2 samples were made from pristine solution and 2 samples from solution with *n*-octylthiol. One sample from each pair was later thermally annealed on the hotplate at 120 °C for several minutes. During all measurements the samples were kept at room temperature. For visualization of the postproduction treatment and alkyl thiol addition effects the experiments were performed for all four fabricated bulk-heterojunction solar cells. To finalize the preparation of solar cell, the top electrode consisting of 0.5 nm LiF and subsequently Al was evaporated in the vacuum below 10^{-5} mbar. The size of the active area of the solar cells was between 3 mm^2 and 12 mm^2.

For film preparation spincoater obtained from Specialty Coating Systems Inc. model P6700 was used. Optical absorption spectra and absorption coefficient were measured using Cary 3G UV–Visibile Spectrophotometer and film thickness (as well as film morphology) was determined Veeco Nanoscope DI 3100 AFM. Current–voltage curves were measured with a Keithley SMU 236 in the dark and under an illumination intensity of 1000 Wm^{-2} with a Steuernagel Lichttechnik GmbH solar simulator providing the AM1.5 sun spectrum. In the IPCE measurements were using standard setup. During the CELIV measurement the triangle-shaped voltage pulses were generated using Agilent 33250A arbitrary pulse generator controlled by Stanford Research Systems DG535 pulse generator. In the photo-CELIV measurements Coherent Infinity 40–100 Nd:YAG 5ns 532 nm laser was used together with supporting optics. Custom written Labview control program controlled the timing between the laser and triangle voltage pulses.

Acknowledgements

The financial support of Austrian Foundation for Advancement of Science (FWF Project No. S9711-N08) Valuable discussions with Alan Heeger, Dan Moses and G. Bazan is gratefully acknowledged.

References

[1] J. Peet, C. Soci, R.C. Coffin, T.Q. Nguyen, A. Mikhailovsky, D. Moses, G.C. Bazan, Appl. Phys. Lett. 89 (2006) 252105.
[2] J. Peet, J.Y. Kim, N.E. Coates, W.L. Ma, D. Moses, A.J. Heeger, G.C. Bazan, Nat. Mater. 6 (2007) 497.
[3] G.A. Chamberlain, Sol. Cells 8 (1983) 47.
[4] D. Wöhrle, D. Meissner, Adv. Mater. 3 (1991) 129.
[5] C.J. Brabec, N.S. Sariciftci, J.C. Hummelen, Adv. Funct. Mater. 11 (2001) 15.
[6] J.J.M. Halls, R.H. Friend, in: M.D. Archer, R. Hill (Eds.), Imperial College Press, London, UK, 2001.
[7] J. Nelson, Curr. Opinion. Solid State Mater. Sci. 6 (2002) 87.
[8] J.-M. NunziC.R. Physique 32002 523.
[9] W. Ma, C. Yang, X. Gong, K. Lee, A.J. Heeger, Adv. Funct. Mater. 15 (2005) 1617.
[10] Y. Kim, S. Cook, S.M. Tuladhar, S.A. Choulis, J. Nelson, J.R. Durrant, D.D.C. Bradley, M. Giles, I. Mcculloch, C.-S. Ha, M. Ree, Nat. Mater. 5 (2006) 197.
[11] S.E. Shaheen, C.J. Brabec, N.S. Sariciftci, Appl. Phys. Lett. 78 (2001) 841.
[12] H. Hoppe, N.S. Sariciftci, J. Mater. Chem. 16 (2006) 45.
[13] H. Hoppe, N.S. Sariciftci, J. Mater. Res. 19 (7) (2004).
[14] X. Yang, J. Loos, S.C. Veenstra, W.J.H. Verhees, M.M. Wienk, J.M. Kroon, M.A.J. Michels, R.A.J. Janssen, Nano. Lett. 5 (4) (2005) 579.
[15] H. Sirringhaus, P.J. Brown, R.H. Friend, M.M. Nielsen, K. Bechgaard, B.M.W. Langeveld-Voss, A.J.H. Spiering, R.A.J. Janssen, E.W. Meijer, P. Herwig, D.M. de Leeuw, Nature 401 (1999) 685.
[16] R. Österbacka, C.P. An, X.M. Jiang, Z.V. Vardeny, Science 287 (5454) (2000) 839.
[17] S. Berson, R. De Bettignies, S. Bailly, S. Guillerez, Adv. Func. Mater. 17 (2007) 1377.
[18] G. Yu, J. Gao, J.C. Hummelen, F. Wudl, A.J. Heeger, Science 270 (1995) 1789.
[19] Y. Kim, S.A. Choulis, J. Nelson, D.D.C. Bradley, S. Cook, R. Durrant, Appl. Phys. Lett. 86 (2005) 063502.
[20] G. Li, V. Shrotriya, J. Huang, Y. Yao, T. Moriarty, K. Emery, Y. Yang, Nat. Mater. 4 (2005) 864.
[21] P. Vanlaeke, G. Vanhoyland, T. Aernouts, D. Cheyns, C. Deibel, J. Manca, P. Heremans, J. Poortmans, Thin Solid Films 511 (2006) 358.
[22] V.D. Mihailetchi, H. Xie, B. de Boer, L.M. Popescu, J.C. Hummelen, P.W.M. Blom, L.J.A. Koster, Appl. Phys. Lett. 89 (2006) 012107.
[23] K. Kim, J. Liu, D.L. Carroll, Appl. Phys. Lett. 88 (2006) 181911.
[24] F. Padinger, R.S. Rittberger, N.S. Sariciftci, Adv. Funct. Mater. 13 (2003) 1.
[25] A.J. Moulé, K. Meerholz, Adv. Mater. 20 (2008) 240.
[26] S. Cook, A. Furube, R. Katoh, Jap. J. Appl. Phys. 40 (2008) 1238.
[27] D. Chirvase, J. Parisi, J.C. Hummelen, V. Dyakonov, Nanotechnology 15 (2004) 1317.
[28] G. Li, V. Shrotriya, Y. Yao, Y. Yang, J. Appl. Phys. 98 (2005) 043704.
[29] I. Riedel, V. Dyakonov, Phys. Status Solidi (A), Appl. Res. 201 (6) (2004) 1332.
[30] M.R. Reyes, K. Kim, D.L. Carroll, Appl. Phys. Lett. 87 (2005) 083506.
[31] A. Rose, Phys. Rev. 97 (1955) 1538.
[32] G. Juška, K. Arlauskas, M. Viliūnas, J. Kočka, Phys. Rev. Lett. 84 (2000) 4946.
[33] A. Pivrikas, R. Osterbacka, G. Juska, K. Arlauskas, H. Stubb, Synthetic Met. 155 (2005) 15.
[34] S.C. Jain, W. Geens, A. Mehra, V. Kumar, T. Aernouts, J. Poortmans, R. Mertens, M. Willander, J. Appl. Phys. 89 (2001) 3804.
[35] V.I. Arkhipov, H. von Seggern, E.V. Emelianova, Appl. Phys. Lett. 83 (2003) 5074.

[36] R. Österbacka, A. Pivrikas, G. Juška, K. Genevičiusb, K. Arlauskas, H. Stubb, Curr. Appl. Phys. 4 (2004) 534.
[37] G. Juška, K. Genevičius, K. Arlauskas, R. Österbacka, H. Stubb, Phys. Rev. B 65 (2002) 233208.
[38] H. Bässler, Phys. Status Solidi (B), Basic Res. 175 (1993) 15.
[39] S.V. Novikov, D.H. Dunlap, V.M. Kenkre, P.E. Parris, A.V. Vannikov, Phys. Rev. Lett. 81 (1998) 4472.
[40] G. Juška, K. Genevičius, G. Sliaužys, A. Pivrikas, M. Scharber, R. Österbacka, J. Appl. Phys. 101 (2007) 114505.